

# Room-temperature surface-assisted reactivity of a melanin precursor: silver metal-organic coordination *versus* covalent dimerization on gold

F. De Marchi,<sup>a,†</sup> G. Galeotti,<sup>a,†</sup> M. Simenas,<sup>b</sup> E. E. Tornau,<sup>c</sup> A. Pezzella,<sup>d,e</sup> J. MacLeod,<sup>f,\*</sup> M. Ebrahimi,<sup>a,\$,\*</sup> F. Rosei<sup>a,g\*</sup>

<sup>a</sup> Centre Energie, Matériaux et Télécommunications, Institut National de la Recherche Scientifique, 1650 Boulevard Lionel-Boulet, Varennes, QC, Canada J3X 1S2;

<sup>b</sup> Faculty of Physics, Vilnius University, Saulėtekio 9. LT-10222 Vilnius, Lithuania;

<sup>c</sup> Semiconductor Physics Institute, Center for Physical Sciences and Technology, Saulėtekio 3, LT-10222 Vilnius, Lithuania;

<sup>d</sup> Institute for Polymers, Composites and Biomaterials (IPCB), CNR, Via Campi Flegrei 34, I-80078 Pozzuoli (NA), Italy;

<sup>e</sup> National Interuniversity Consortium of Materials Science and Technology (INSTM), Florence 50121, Italy;

<sup>f</sup> School of Chemistry, Physics and Mechanical Engineering and Institute for Future Environments, Queensland University of Technology (QUT), 2 George Street, Brisbane, 4001 QLD, Australia;

<sup>g</sup> Institute for Fundamental and Frontier Science, University of Electronic Science and Technology of China, Chengdu 610054, PR China;

<sup>†</sup> The authors contribute equally;

<sup>\$</sup> Current address: Physics Department E20, Technical University of Munich, James-Frank-Str.1, D-85748 Garching, Germany;

\* Corresponding authors' e-mail: [jennifer.macleod@qut.edu.au](mailto:jennifer.macleod@qut.edu.au), [maryam.ebrahimi@emt.inrs.ca](mailto:maryam.ebrahimi@emt.inrs.ca), [rosei@emt.inrs.ca](mailto:rosei@emt.inrs.ca);

## Contents

<a href="#">DHI/Ag(111) – STM</a> .....	2
<a href="#">DHI/Ag(111) – XPS</a> .....	4
<a href="#">DHI/Ag(111) – DFT model for DHI-Ag-IQ</a> .....	6
<a href="#">DHI/Ag(111) – MC model</a> .....	7
<a href="#">DHI/Ag(111) – TOF-SIMS</a> .....	9
<a href="#">DHI/Au(111) – STM</a> .....	10
<a href="#">DHI/Au(111) – XPS</a> .....	11
<a href="#">DHI/Au(111) – DFT simulations for DHI dimer</a> .....	11

## DHI/Ag(111) – STM

After deposition on Ag(111), DHI forms extended domains, with dimensions up to hundreds of nanometers, (Figure S1). For lower coverage, DHI still organizes in lamellae, with increased spacing (Figure S2b). At very low coverage, it is possible to find single lamellae on the surface, but their imaging is difficult due to molecular diffusion (figure S2a).

Even for full monolayers, it is often possible to observe some lamella with different contrast or orientation within the domains (Figure S1 and S3). These variations are probably due to the presence of a pure DHI lamella, with the dimensions and geometry that are different from the IQ/DHI lamella.

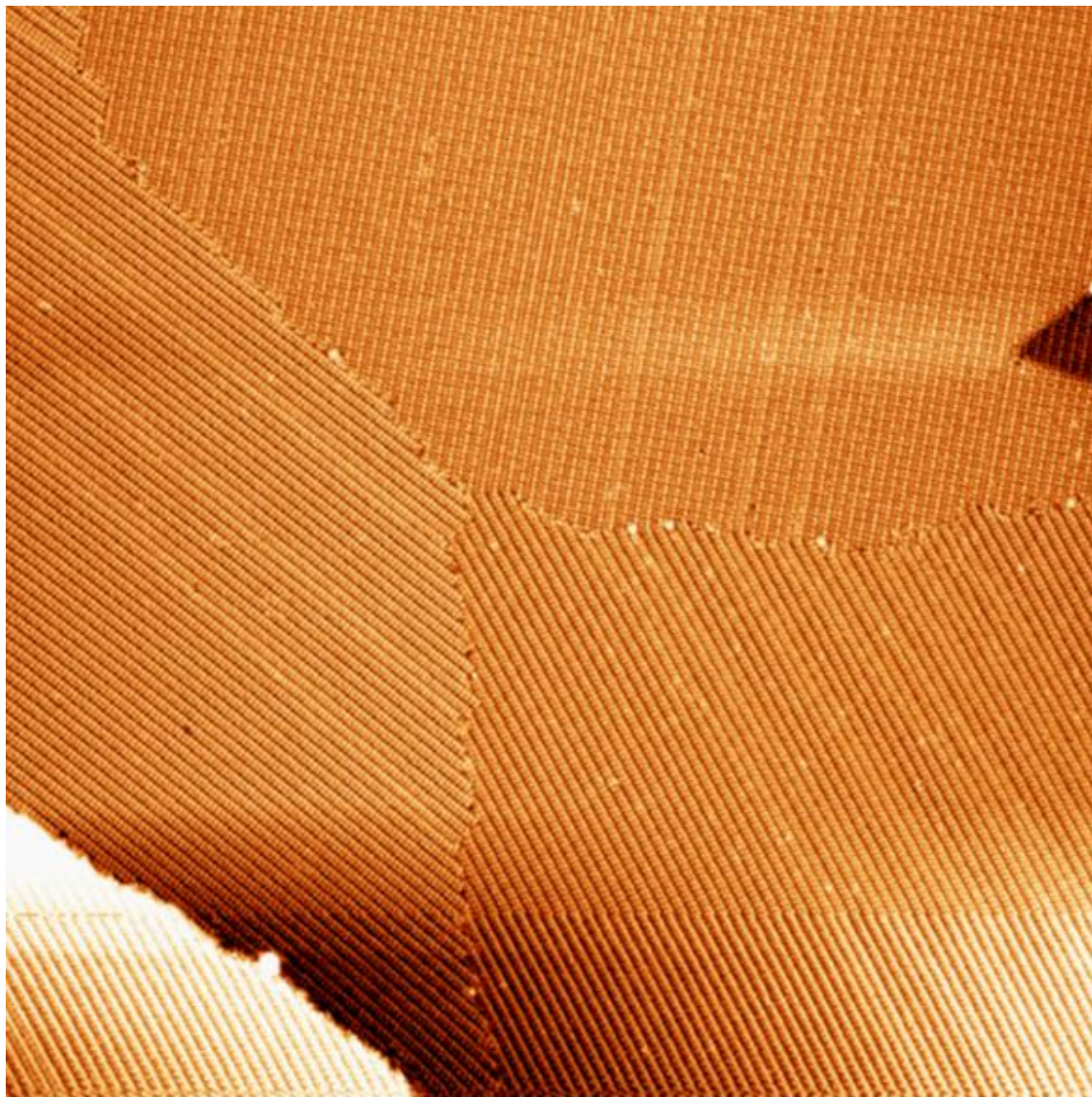


*Figure S1: Large scale image of the DHI /Ag111 lamellar phase (0.23 nA, 0.51 V, 170x170 nm<sup>2</sup>)*



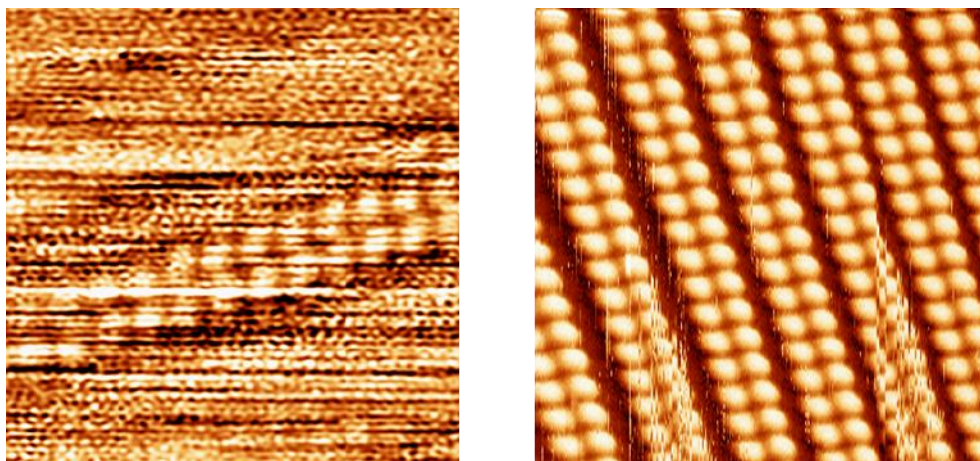


Figure S2: Different lamellar phases of DHI/Ag111, obtained at coverages lower than 1 ML. a) (0.1 nA, -0.5 V, 8x8 nm<sup>2</sup>) b) (0.11 nA, -0.52 V, 12x12 nm<sup>2</sup>)

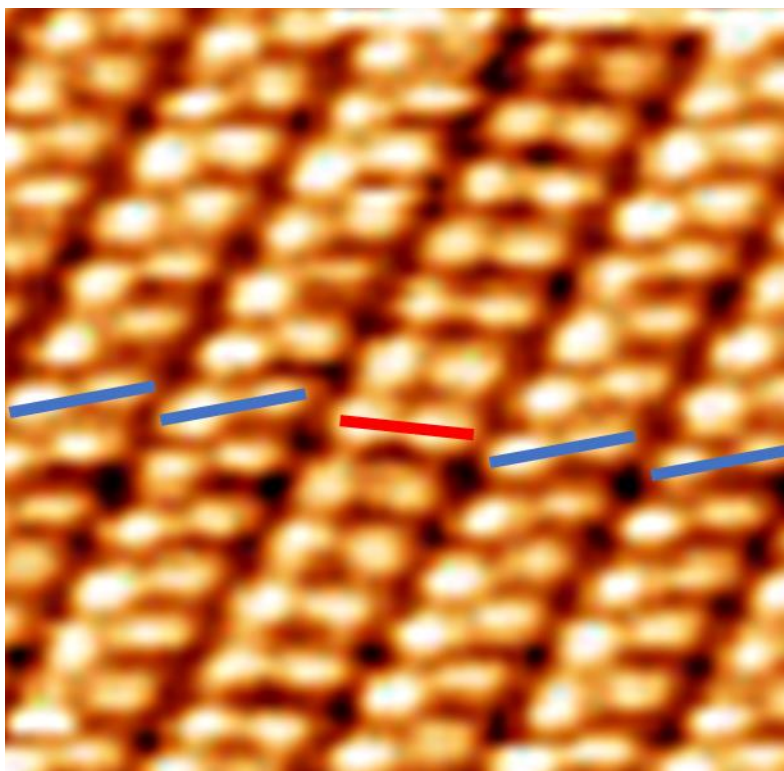


Figure S3: Pure DHI lamella (in red) surrounded by DHI/IQ lamellae (0.2 nA, -0.51 V, 10x10 nm<sup>2</sup>). The dimers are overlaid with short lines, to underline the different orientation of the lamella with respect to their neighbors.

## DHI/Ag(111) – XPS

The peak position of the fitted XPS spectra of the DHI/Au and DHI/Ag systems are reported in Table S1. For the purpose of peak fitting, the value of each FWHM was not fixed but it was left free to vary within a reasonable range (Table S2) to reflect the different bonding environments due to the chemical/structural diversity of the system. After the exposure to O<sub>2</sub>, the difference in peak widths strongly increases (2.35 eV vs 1.77 eV) and reflects the disorder of the sample: the FWHM of the O-C component gets larger to reflect the multiple bonding pattern that the molecule adopts across the surface.

Table S1: Peak position of the fitted XPS spectra in figures 3, 5 and 8 of the main manuscript.

		Ag(111)		Au(111)
		As deposited	After O2	As deposited
O1s	C-OH	533.0	532.8	533.0
	C=O	531.0	531.2	-
	O-Ag	-	530.1	-
C1s	C-C	284.6	284.1	284.5
	C-N	285.3	255.0	285.0
	C-OH	285.9	285.8	285.9
	C=O	288.7	287.8	-

Table S2: FWHM of the fitted peaks in figures 3, 5 and 8 of the main manuscript.

		Ag(111)		Au(111)
		As deposited	After O2	As deposited
O1s	C-OH	1.94	2.00	2.0
	C=O	1.66	2.00	-
	O-Ag	-	1.49	-
C1s	C-C	1.40	1.53	1.67
	C-N	1.35	1.27	1.38
	C-OH	1.61	1.42	1.53
	C=O	2.50	2.50	-

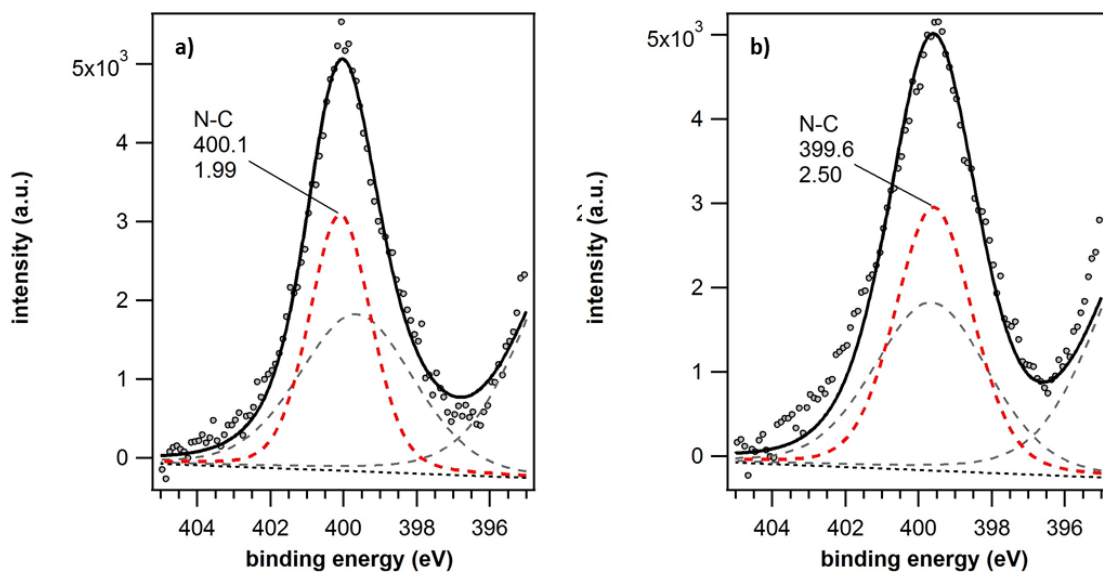


Figure S4: XPS spectra of DHI/Ag(111) a) before and b) after exposure to  $O_2$ . The displayed grey component accounts for the spectral weight contributed by the clean substrate.

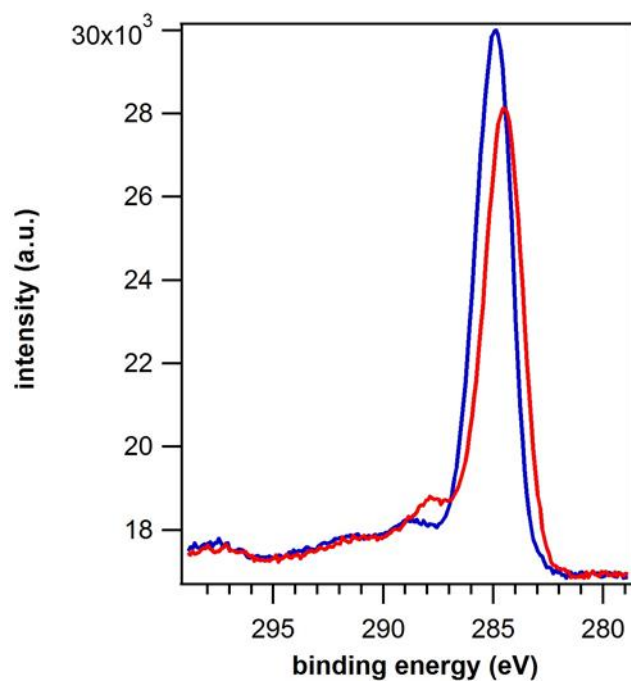


Figure S5: Comparison of the C 1s spectra of the DHICA/Ag111 before (blue) and after (red)  $O_2$  exposure

## DHI/Ag(111) – DFT model for DHI-Ag-IQ

We simulated different possible configurations of the metal-organic DHI dimer. Since we have not been able to identify the commensurate unit cell associated with the observed metal-organic molecular structure, a simulation of a proper model, with a supercell containing both the metal-organic structures and the surface representing the SAMNs observed in our experimental data, was not feasible due to the limitation imposed by PBC. Nevertheless, to explore a more advanced model, we included the surface in the DFT simulation, in which the proposed metal-organic structure would be stabilized due to the interaction with surface atoms.

Based on the starting position of the hydrogen on the hydroxyl groups, the simulation converges towards the formation of a linear dimer (as shown in Figure S6a), or a more asymmetrical one (Figure S6d). In both cases, IQ is located at a closer distance to the substrate to maintain a coordination with the Ag adatom (Figure S6c & f), and the silver adatom lies closer to the oxygens of IQ than those of DHI.

The linear dimer displays an angle  $\theta$  between the carbons in position 2 and the silver to be equal to  $176.7^\circ$  (vs the experimental value of  $172 \pm 5^\circ$ ), and the silver adatom lies almost perfectly in between the IQ oxygens ( $O \cdots Ag = 2.34 \text{ \AA}$  &  $2.37 \text{ \AA}$ ) and the DHI ones ( $HO \cdots Ag = 2.63 \text{ \AA}$  &  $2.81 \text{ \AA}$ ).

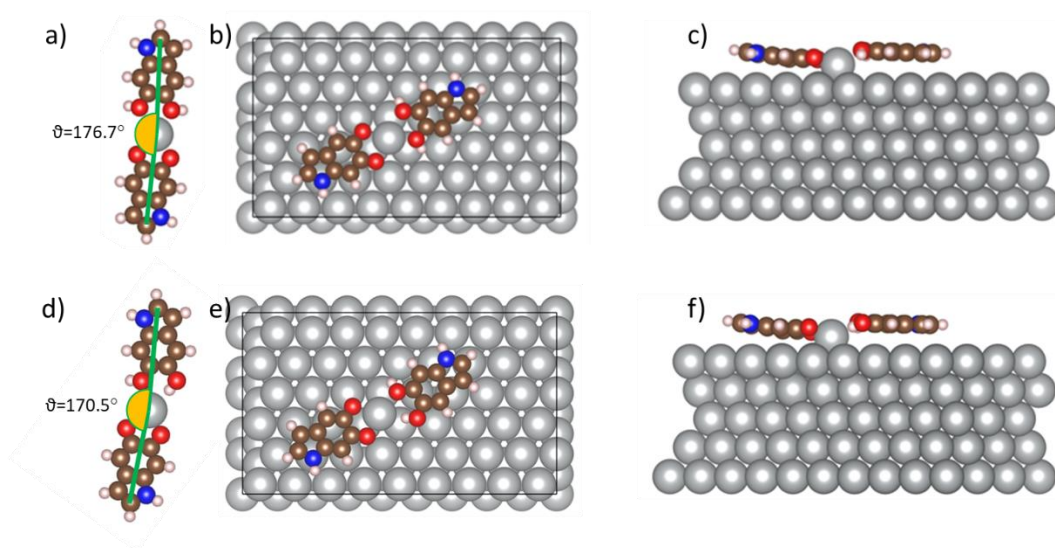


Figure S6: Top-view and side-view of DFT simulated structures of one metal-organic DHI-Ag-IQ dimer with (a-c) symmetric and (d-f) asymmetric alignment on a 5-layer Ag(111) slab of 270- silver atoms.

In the asymmetric configuration, one of the hydrogens of hydroxyl group locates in a closer distance to the silver adatom than its corresponding hydroxyl oxygen, leading to a dimer with an angle  $\theta$  equal to  $170.5^\circ$ . The silver adatom coordinates with only one of the catechol oxygens ( $HO \cdots Ag = 2.64 \text{ \AA}$  &  $3.38 \text{ \AA}$ ) and also a minor asymmetry is present in the Ag position compared to the quinone oxygens ( $O \cdots Ag = 2.36 \text{ \AA}$  &  $2.29 \text{ \AA}$ ). The two models have very similar energy within  $\Delta E = 0.01 \text{ eV}$  difference which is well below the  $kT$  value at room temperature. The simulation of two dimers (Figure S7) gave an energy difference of  $\Delta E = 0.10 \text{ eV}$  between the linear and asymmetric structures, with the latter configuration being more stable.



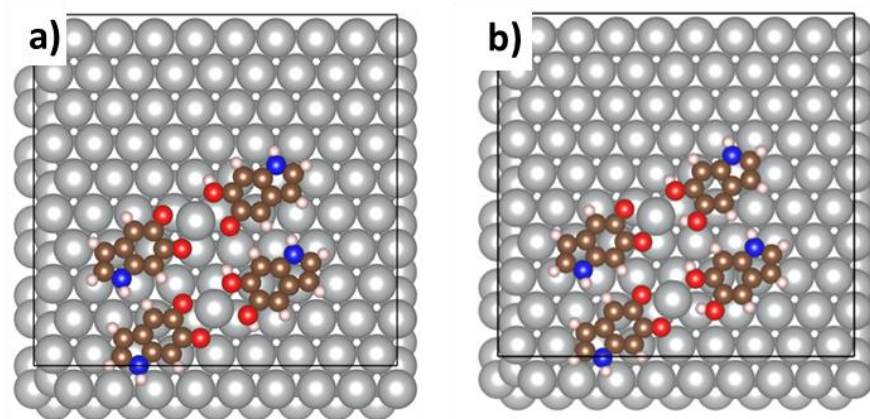


Figure S7: DFT simulated structures of two DHI-Ag-IQ dimers in the a) linear and b) asymmetric configurations.

We have superimposed both the linear and asymmetric metal-organic dimers with the STM image in Figure S8, showing that while both the proposed DHI-Ag-IQ models match the experimental data in terms of the dimension, the asymmetric one better fits the molecular features of the image (as shown below in Figure S8).

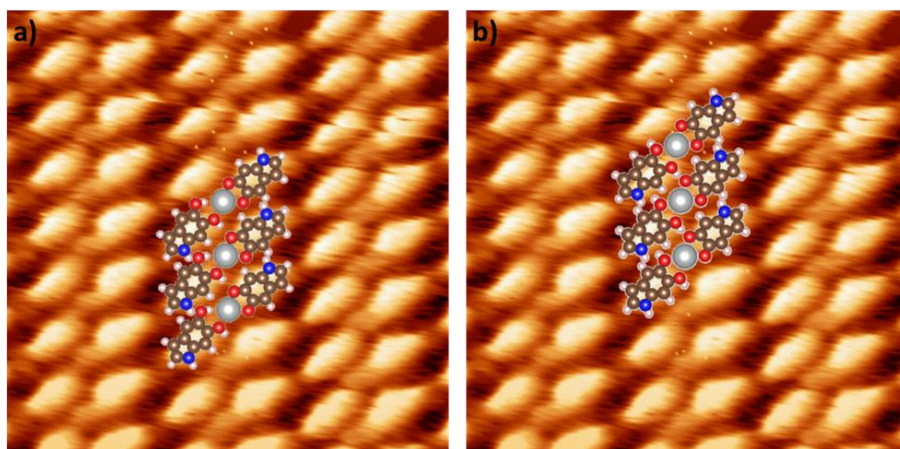


Figure S8: a) Overlay of the simulated DHI-Ag-IQ dimer over the STM image. b) detail of the DHI-Ag-IQ metal-organic dimer.

## DHI/Ag(111) – MC model

In the MC model, the center of the DHI molecule (and its rotation axis) is assumed to occupy one site of a square lattice as shown in Figure 6. The molecule is assumed to have four molecular states which differ in  $90^\circ$  rotation of a molecule (Figure 6, left). The fifth state is a vacancy state (no molecule on a site). The molecule is free to move over the sites of the lattice and rotate to one of the four mentioned states. There are three intermolecular interactions that drive the ordering in the model (Figure 6a).

We note that for simplicity, the Ag adatoms in our model act as interaction mediators and are not explicitly considered. We also ignored the chiral nature of the DHI molecules, as nitrogen atom barely affects the side interactions (DFT calculations for gas-phase using B3LYP D3 6-31G(d,p) reveals a difference of 0.11 kcal/mol between the different configurations). Additionally, the side interactions are the same for the catechol and quinone molecules.

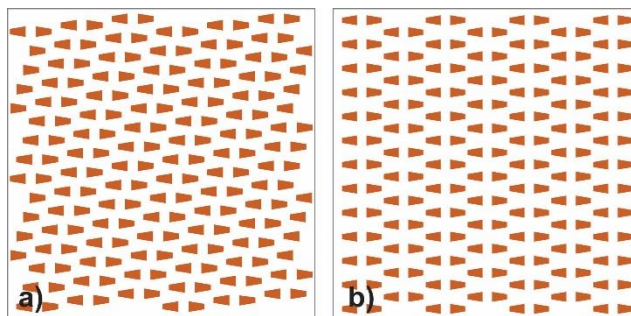


Figure S9: Snapshots of MC simulations obtained for a)  $e_{s1} < e_{s2}$  (experimental structure) and b)  $e_{s1} > e_{s2}$ . Other simulation parameters:  $e_d = 1$ ,  $T = 0.1$ .

## DHI/Ag(111) – TOF-SIMS

Reported in Figure S10 is the result of the TOF-SIMS measurements on the DHI/Ag(111) sample. As it is evident from Figure S8b, no peak is visible for mass close to DHI dimer. On the other hand, several peaks are present at mass 149.15 and lower. These peaks are related to DHI and IQ, and to their deprotonated counterparts. (Figure S8a).

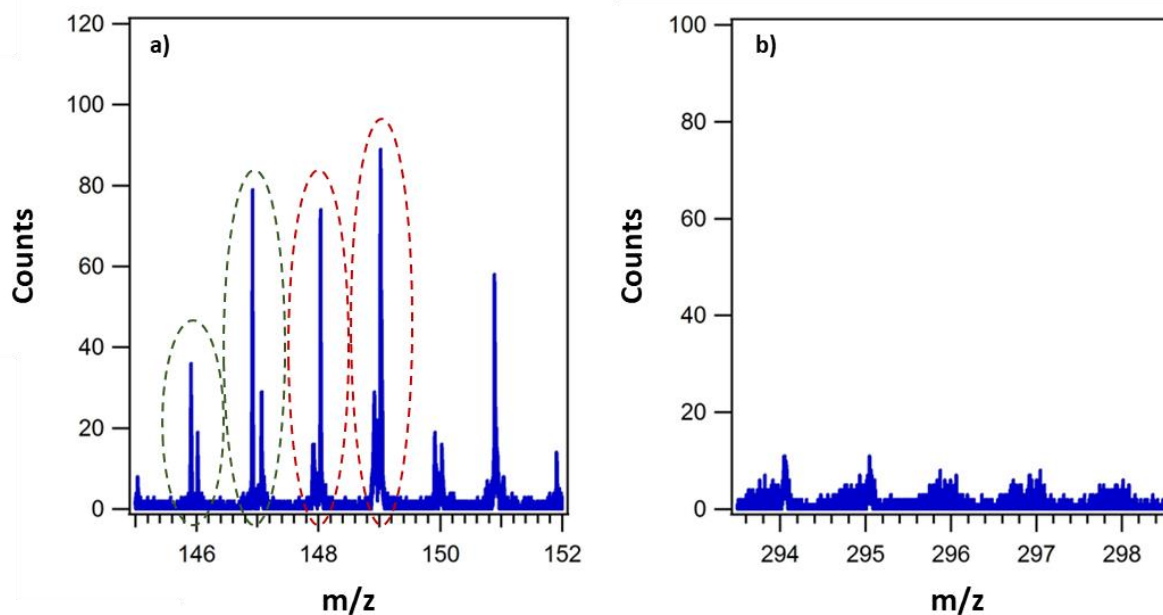


Figure S10: Detail of the TOF-SIMS analysis of the DHI/Ag sample. a) shows the region around the monomer mass, where the peaks associated with DHI (in red-dash) and IQ (in green-dash) are highlighted. b) No peak associated with dimer species is detected.



## DHI/Au(111) – STM

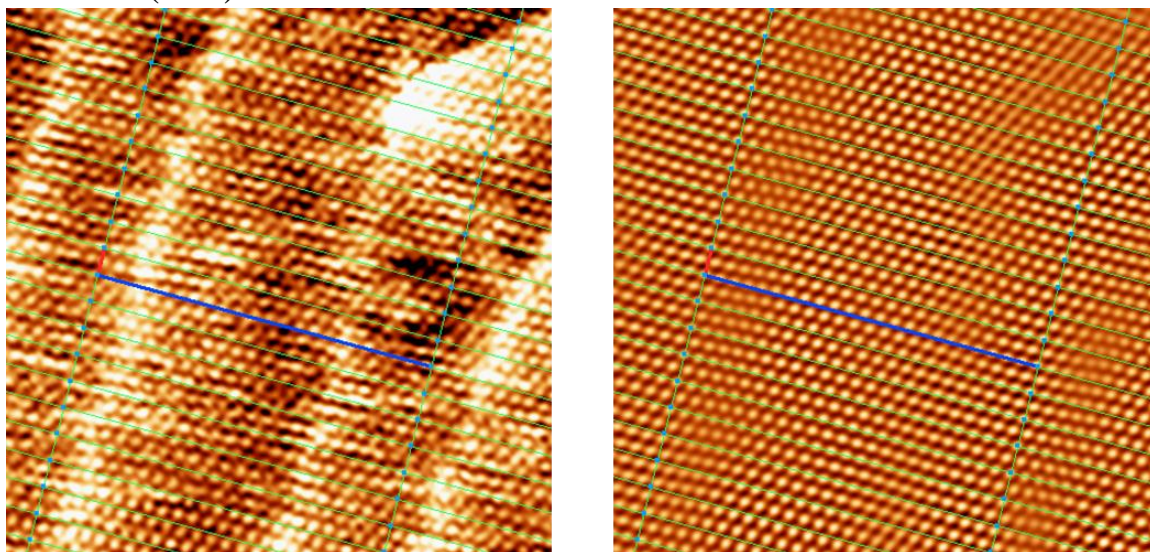


Figure S11: an example of the calibration adopted for the DHI/Au(111) phase, where the clean Au substrate image. (3.30 nA, 0.01 V, 10x10 nm<sup>2</sup>) has been processed and filtered until the single atoms are properly visible. The image has been calibrated by using the 6.23 nm herring bone reconstruction dimension (1-10, blue vector in the image) at 90° respect to the direction of the solitons (112, red vector in the image) as the distance between 23 atoms.

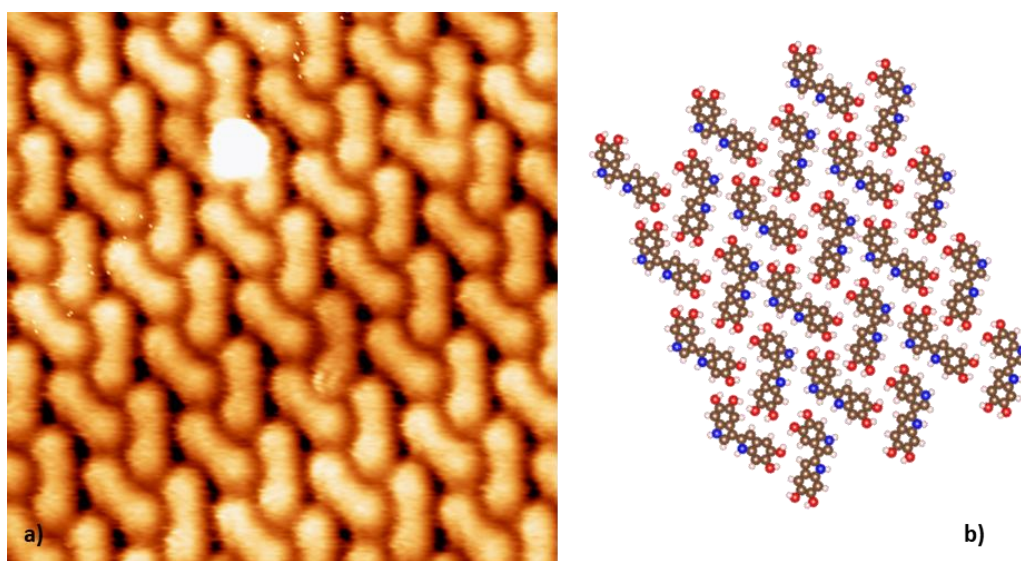


Figure S12: The banana shaped dimers occasionally adopted a different conformation, with identical lattice dimensions, but with one of the dimer in its mirror geometry respect to the common case, as depicted in the a) STM image (1.20 nA, 0.20 V, 8x8 nm<sup>2</sup>). b) A proposed molecular structure for this phase.

## DHI/Au(111) – XPS

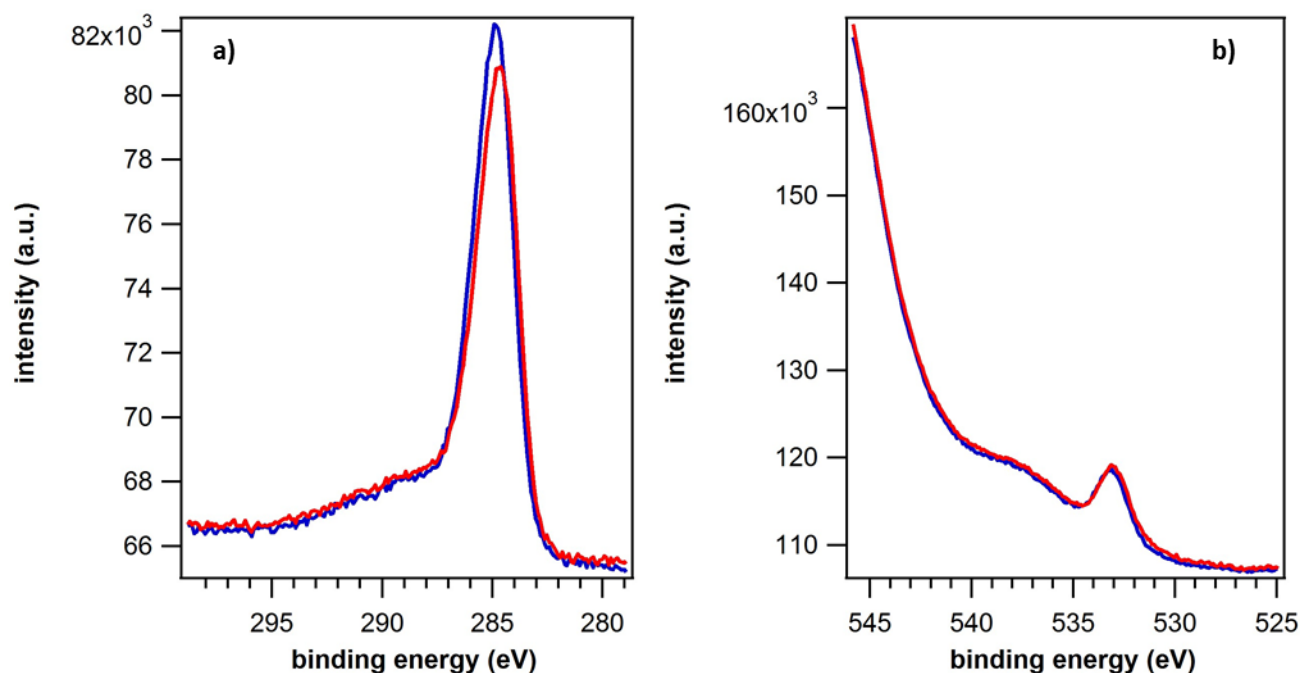


Figure S13: Comparison of the a) C 1s spectra and b) O1s before (blue) and after (red) O<sub>2</sub> exposure

## DHI/Au(111) – DFT simulations for DHI dimer

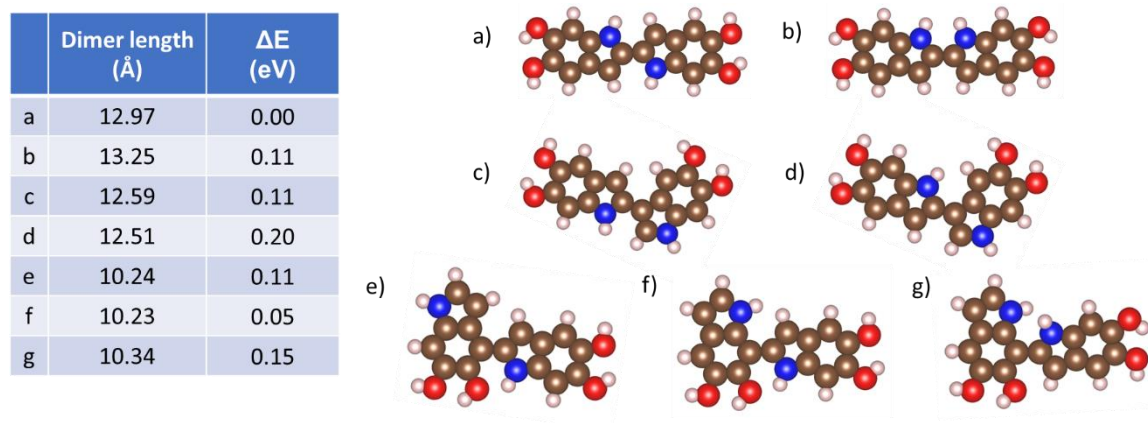


Figure S14: Possible regioisomers for a planar DHI dimer. The table reports the length of the dimer in Å, calculated as the distance between the two farthest atoms, and the energetic difference respect to the dimer (a). The dimers a-b (linear-shape) do not fit the banana-shape. Both dimers c-d (banana-shape) similarly fit the imaged features, while dimers e-g (T-shape) do not match the experimental data. The difference of the free energy of each structure (DFT calculation by the described method in the MS) with respect to the most energetically stable dimer structure (a) is reported, all of which are within the available energy at room-temperature. The dimer structure (c) which best fits the STM imaged features was further simulated in the slab-model (Figure 7, MS).

Table S3: Calculated energies for DHI monomer, dimer, H<sub>2</sub> molecules and the dimerization reactions

Molecule	B3LYP/ basis set:			
	6-311G(d,P)		6-31G(d)	
	eV	kcal/mol	eV	kcal/mol
DHI monomer	-13997.66	-321946.22	-13993.69	-321854.87
SQ monomer	-13963.19	-321153.29	-13959.56	-321069.86
IQ monomer	-13963.57	-321162.18	-13959.98	-320849.43
DHI dimer	-27962.86	-643145.72	-27955.14	-642968.17
H <sub>2</sub>	-32.10	-738.30	-31.99	-735.70
$\Delta E = (\text{dimer} + \text{H}_2) - (2 \times \text{DHI})$	0.37	8.42	0.26	5.87
$\Delta E = (\text{dimer}) - (\text{H}_2 + 2 \times \text{SQ})$	-4.38	-100.84	-4.03	-92.76
$\Delta E = (\text{dimer}) - (\text{H}_2 + 2 \times \text{IQ})$	-3.61	-83.07	-3.20	-73.62

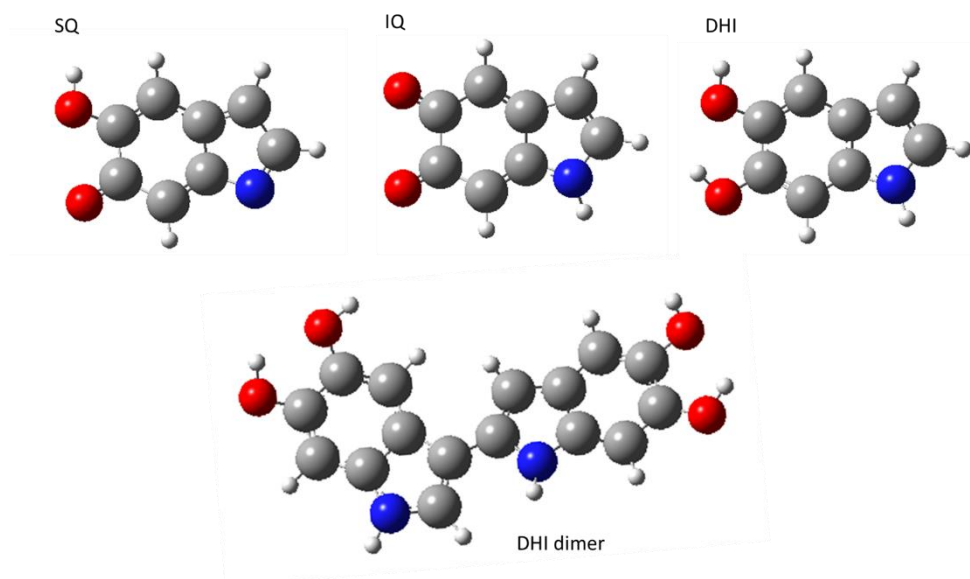


Figure S15: Simulated DFT structures: DHI dimer, DHI and its redox forms, IQ and SQ